Differential Scanning Calorimetric Analysis of Edible Oils: Comparison of Thermal Properties and Chemical Composition

C.P. Tan and Y.B. Che Man*

Department of Food Technology, Faculty of Food Science and Biotechnology, Universiti Putra Malaysia, 43400 UPM Serdang, Malaysia

ABTRACT: The thermal profiles of 17 edible oil samples from different plant origins were examined by differential scanning calorimetry (DSC). Two other confirmatory analytical techniques, namely gas–liquid chromatography (GLC) and high-performance liquid chromatography (HPLC), were used to determine fatty acid (FA) and triacylglycerol (TAG) compositions. The FA and TAG compositions were used to complement the DSC data. Iodine value (IV) analysis was carried out to measure the degree of unsaturation in these oil samples. The DSC melting and crystallization curves of the oil samples are reported. The contrasting DSC thermal curves provide a way of distinguishing among these oil samples. Generally, the oil samples with a high degree of saturation (IV < 65) showed DSC melting and crystallization profiles at higher temperature regions than the oil samples with high degree of unsaturation (IV > 65). Each thermal curve was used to determine three DSC parameters, namely, onset temperature (T_o), offset temperature (T_f) and temperature range (difference between T_o and T_f). Reproducibility of DSC curves was evaluated based on these parameters. Satisfactory reproducibility was achieved for quantitation of these DSC parameters. The results show that T_o of the crystallization curve and T_f of the melting curve differed significantly ($P < 0.01$) in all oil samples. Our observations strengthen the premise that DSC is an efficient and accurate method for characterizing edible oils.

Paper no. J9207 in *JAOCS 77*, 143–155 (February 2000).

KEY WORDS: Crystallization, differential scanning calorimetry, edible oil, fatty acid composition, gas chromatography, high-performance liquid chromatography, melting, thermal properties, triacylglycerol composition.

The importance of oils and fats as valuable commodities in world trade and for human nutrition is well recognized. Oils and fats used for edible purposes are of either plant or animal origin. Compared to those of animal origin, oils and fats from plant origin contain higher proportions of unsaturated fatty acids (FA) and meet the dietary requirements of essential FA (1). This is the main reason for the continued trend in the direction of food products prepared from vegetable oils and away from those prepared from animal fats (2). More than 100 varieties of plants are known to have oil-bearing seeds, but only a few have been commercialized (3). At present, the major sources of vegetable oil are seeds of annual plants such as canola, corn, peanut, safflower, soybean, and sunflower. A second rich source of vegetable oils is the oil-bearing fruits and nuts of trees such as coconut, palm, palm kernel, and olive.

Every oil or fat has characteristic FA and triacylglycerol (TAG) profiles, which are unique to the type of oil and can be used in detecting adulteration (4). In general, all oils and fats are composed of a complex mixture of 96 to 99% of TAG, which are the esters of glycerol and FA. Therefore, oils and fats from plant origin can be further classified according to their FA and TAG compositions. The principal variation in FA composition of oils and fats is the chainlength and degree of unsaturation of the component FA (5). This variation in FA composition can dramatically affect the bioavailability and digestibility of oils and fats in infants and adults (1). It is relatively easy to analyze the constituent FA of an oil or fat. The percentage distribution of different FA in a sample can be obtained by gas–liquid chromatography (GLC) technique. Analysis of the TAG composition of an oil or fat requires methods of separating their complex mixtures into individual components or at least into simpler mixtures that contain only a few TAG each (6). The complex mixtures of TAG from oils and fats have usually been analyzed by reversed-phase high-performance liquid chromatography (HPLC) (7). The TAG composition data are more likely to be characteristic of a given type of oil or fat because they contain structural information, for example, the position of the FA residues on the glycerol backbone, information that is lost on transesterification necessary for FA analysis by GLC (8). However, complete determination of TAG profile can be achieved only by several successive procedures that are tedious and time-consuming (9). Therefore, this approach is less practical for the oil industry, for quality-control programs, and for many research and development programs.

Thermal analysis has long been available to the oils and fats researcher (10). Since applications of this technique started, an abundance of data has become available on the reproducibility of some basic quantities measured or derived from thermoanalytical curves (11). Differential scanning calorimetry (DSC) is the most widely used thermoanalytical technique for oils and

*To whom correspondence should be addressed.
E-mail: yaakub@fsb.upm.edu.my.

fats (12). This technique is used for studying various heat-related phenomena in materials by monitoring associated changes in enthalpy. Nowadays, DSC is preferred to other similar calorimetric techniques, such as differential thermal analysis, because the former has the advantage of providing a more direct measurement of the energy accompanying the physical and chemical changes studied (13). For many years, DSC data of oils and fats have given valuable information on melting and crystallizing temperatures as well as heats of fusion and crystallization (14). This technique has been used for monitoring phase behavior of TAG mixtures (15), for evaluating the effects of minor components on the crystallization of oils and fats (12), for observing polymorphic transformations in edible oils and fats (16), and also for monitoring failed-batch palm oil (17). Application of statistical and mathematical techniques to DSC data can be used to measure fat solids (18), to determine the country of origin of the oil-bearing nut (19), to detect adulterants in animal fats and butter (20), to estimate the amount of saturation present in transesterified blends of jojoba wax esters (21), and to quantify the iodine value (IV) in palm oil (22). Most recently, we (23) used these techniques to determine total polar compounds in heated oils.

Heat-related phenomena in oils and fats are fundamental and can be used to elucidate their physical and chemical properties. The complexity of the thermal profiles of oils and fats is essentially due to the great variety of TAG as their principal constituents (24). Therefore, oils and fats do not have specific melting and crystallization temperatures. Rather, they show melting/crystallization profiles. In the DSC melting curves of oils and fats, complex features were not easily interpretable (25). This is a consequence of the known phenomenon of polymorphism of oils and fats that is strongly dependent on the thermal history of the sample. Conversely, the DSC crystallization curve, which is influenced only by the chemical composition of the sample, and not by the initial crystalline state, is more reproducible and simpler than the melting curve (23). Many studies have been conducted to investigate the thermal profile of various oils and fats products (24,26). Most recently, Che Man and co-workers (27) have studied the thermal profile of crude palm oil and its products. Although information has been published concerning the thermal profile of most edible oils and fats, it is often difficult to compare data from various sources because of a lack of uniformity of analytical techniques used in qualitative or quantitative analysis. In light of this knowledge, investigations reported herein were directed toward obtaining basic information about the relationship between the thermal profile and chemical composition of 17 different edible oils and fats.

MATERIALS AND METHODS

Materials and treatments. Different edible oils (n = 17) from various plant origins were used in this study. Refined-bleached-deodorized palm oil (RBDPO), refined-bleached-deodorized palm stearin ($RBDPO_S$), and palm kernel oil (PKO) were obtained from a local refinery. The other samples were purchased from several local retailers. These oils and fats were divided into three major groups for more consistency in the discussion. All chemicals and solvents used were Analar or HPLC grades (Merck, Darmstadt, Germany). Fatty acid methyl esters (FAME) and TAG standards were obtained from Sigma Chemical Co. (St. Louis, MO).

IV analysis. The AOCS Official Method was employed for determinations of iodine value (IV) in the oil samples (28).

FA analysis by GLC. The FA compositions of the oil samples were analyzed with GLC after transesterification. FAME were prepared by transesterification of oil (50 mg) with petroleum ether (0.8 mL) and sodium methoxide (1 M, 0.2 mL) and analyzed on a Hewlett-Packard model 5890 instrument (Palo Alto, CA), equipped with a flame-ionization detector (FID) and a Hewlett-Packard model 3392A integrator. A polar capillary column BPX70 (0.32 mm internal diameter, 30 m length and 0.25 μm film thickness; SGE International Pty. Ltd., Victoria, Australia) was used at a column head pressure of 10 psi. Helium (99.995%) at approximately 23 mL/min (measured at oven temperature 150°C) was used as the carrier gas, and nitrogen (99.999%) at 20 mL/min was used as the makeup gas. The FID and injector temperatures were both maintained at 220°C. The injection mode was splitless, and samples of about 1 μL were injected with a 10-μL loop. The initial column oven temperature was 115°C, temperature was programmed to 180°C at 8°C/min and held at this temperature until the analysis was completed. FAME peaks were identified by comparison of retention times to a standard mixture. The peak areas were computed, and percentages of FAME were obtained as area percentages by direct normalization. (The data are expressed as normalized percentage of all identified FAME). Only the more abundant FA (>0.2%) were considered. All analyses were carried out in triplicate.

TAG analysis by HPLC. The TAG were separated by reversed-phase HPLC with a Waters (Milford, MA) chromatography system, consisting of a Waters 600 controller, coupled with a Waters 410 differential refractometer and a software interface (Millennium 2010 Chromatography Manager Software; Millipore Co., Milford, MA) for processing of the acquired data. The column used was Waters Nova Pak C-18 (3.9 × 300 mm, 60 Å, 4 μm) and maintained at 30°C by a column oven. Sensitivity was set at 16, and the scale factor at 20. Isocratic elution was carried out at a flow rate of 1 mL/min with a mixture of acetone/acetonitrile (63.5:36.5, vol/vol) as the mobile phase. The injection volume was 10 μL of 5% (wt/vol) oil in chloroform. TAG were separated according to their degree of unsaturation and molecular weight. TAG peaks were identified based on the retention time of TAG standards and results of Haryati *et al.* (29), Stefanoudaki *et al.* (30), Bland *et al.* (9), Singleton and Pattee (31), Dong and DiCesare (6), and Parcerisa *et al.* (32). The TAG data were treated as percentage areas. Separated TAG peaks with an area below 0.1% were not integrated. Quantification was carried out by normalization. Each sample was chromatographed three times, and the data are reported as percentage areas.

Thermal analysis by DSC. For DSC analysis, a PerkinElmer differential scanning calorimeter, DSC-7, equipped with a ther-

mal analysis data station (PerkinElmer Corp., Norwalk, CT) was used. Nitrogen (99.999% purity) was the purge gas and flowed at ~20 mL/min. The DSC instrument was calibrated with indium (m.p. 156.6°C, ΔH_f = 28.45 J/g) and *n*-dodecane (m.p. –9.65°C, ΔH_f = 216.73 J/g). Samples of *ca.* 6–12 mg were weighed into aluminum pans to the nearest 0.1 mg, and covers were hermetically sealed into place. An empty, hermetically sealed aluminum pan was used as reference. Prior to analysis of samples, the baseline was obtained with an empty, hermetically sealed aluminum pan. For practical reasons (based on samples' IV), the cooling and heating profiles of samples were defined by using two different temperature programs. Samples in Group 1 were subjected to the following temperature program: 80°C isotherm for 5 min, cooled at 5°C/min to –80°C and held for 5 min. The same sample was then heated from –80 to 80°C at the same rate. Samples in Groups 2 and 3 were subjected to the following temperature program: sample was melted at 50°C and held for 5 min before cooling to –100°C at the rate of 5°C/min. The samples were again held at this temperature for 5 min before heating to 50°C at the rate of 5°C/min. The manufacturer's software (7 Series/UNIX DSC software library) program was used to analyze and plot the thermal data (33). The thermal melting and crystallization characteristics of each sample in a DSC scan can be indicated by various temperatures. The onset temperature (T_o), the offset temperature (T_f) (points where the extrapolated leading edge of the endotherm/exotherm intersects with the baseline), and the various peak temperatures (temperatures of maximum different heat flow) between T_o and T_f were determined. The melting and cooling temperature ranges were obtained by determining the difference between T_o and T_f. All DSC values reported are the average of four scans.

Statistical analysis. Data were statistically analyzed by one-way analysis of variance (ANOVA) with the SAS software package (34). Duncan's multiple-range test was applied to determine significant differences between means, at a level of $P < 0.05$.

RESULTS AND DISCUSSION

FA compositional and proportional analyses. The FA composition (area %) and IV of 17 edible oils are shown in Tables 1 and 2. The FA composition appeared to be typical for these types of oil samples (2,3). The proportions of saturated (SFA), monounsaturated (MUFA), and polyunsaturated (PUFA) FA data are tabulated in Table 3. The results of statistical tests (Duncan's multiple-range test), comparing the mean difference among these data, are also shown in Table 3. It is now well known that the FA composition depends on the origin of plants. Thus, the differences in SFA, MUFA, and PUFA contents found in this study can be easily explained. RBDPO, refined, bleached, and deodorized palm superolein ($RBDPO_{SO}$), red palm olein (RPO_O), and $RBDPO_S$ are oil samples obtained from palm pulp. In these oil samples, the SFA accounted for more than 43%, while the MUFA, mainly oleic ($C_{18:1}$) acid, made up about 20–44% of the total FA. The PUFA content ranged from 4–12%, which also indicates the amount of linoleic ($C_{18:2}$) acid. These oils were distinguished from other oils by high levels (38.1–68.3%) of palmitic ($C_{16:0}$) acid. The predominance of this FA was the main reason for the low IV in palm based oil products, as indicated in Table 1. The fractionation of RBDPO into olein and stearin fractions has a significant influence on FA composition. $RBDPO_{SO}$ and $RBDPO_S$ are two main fractions of RBDPO. As shown in Table 1, the $C_{16:0}$ tends to migrate into the $RBDPO_S$. However, the FA composition of $RBDPO_{SO}$ was relatively similar to RBDPO in spite of the fractionation process. Two types of palm olein fractions were used in this study, namely $RBDPO_{SO}$ and RPO_O. These two olein fractions of palm oil showed comparable FA composition. However, RPO_O had a higher oleic ($C_{18:1}$) acid content than $RBDPO_{SO}$. This was evidenced by a higher IV in RPO_O. The FA composition of PKO was closer to that of coconut oil (CtO). PKO is a co-product from palm oil mills. Although PKO and palm oil

TABLE 1
Fatty Acid Composition (area %) and Iodine Value (g of I_2/100 g oil) of Edible Oil Samples[a]

Fatty acid (area %)	Sample							
	RBDPO	$RBDPO_{SO}$	RPO_O	$RBDPO_S$	CtO	PKO	CnO	PtO
6:0					1.4 ± 0.3	0.5 ± 0.1		
8:0					13.5 ± 1.2	6.4 ± 0.6		
10:0					8.7 ± 0.3	5.2 ± 0.2		
12:0	0.5 ± 0.0	0.7 ± 0.0	0.7 ± 0.1	0.4 ± 0.0	51.1 ± 0.5	55.8 ± 0.1		
14:0	1.7 ± 0.0	1.5 ± 0.0	1.7 ± 0.1	2.1 ± 0.1	14.5 ± 0.5	14.7 ± 0.4		
16:0	48.7 ± 0.2	41.6 ± 0.4	38.1 ± 1.4	68.3 ± 0.9	5.5 ± 0.2	5.8 ± 0.2	13.7 ± 0.1	14.1 ± 0.9
16:1								
18:0	3.9 ± 0.0	3.8 ± 0.0	3.4 ± 0.2	4.0 ± 0.3	1.4 ± 0.2	1.3 ± 0.1	2.2 ± 0.0	3.7 ± 0.1
18:1	37.1 ± 0.2	42.0 ± 0.3	44.2 ± 1.1	20.6 ± 0.6	3.3 ± 0.2	8.9 ± 0.3	27.5 ± 0.2	49.1 ± 0.3
18:2	8.1 ± 0.1	10.4 ± 0.1	12.0 ± 0.3	4.6 ± 0.2	0.7 ± 0.2	1.5 ± 0.0	55.7 ± 0.3	27.4 ± 0.6
18:3							0.9 ± 0.0	
20:0								1.6 ± 0.0
20:1								1.0 ± 0.1
22:0								3.0 ± 0.1
Iodine value	53.80 ± 0.19	61.90 ± 0.01	65.03 ± 0.39	32.78 ± 0.28	9.37 ± 0.19	19.30 ± 0.01	129.01 ± 0.47	95.23 ± 0.53

[a]Each value in the table represents the means ± SD of triplicate analyses. Abbreviations: RBDPO, refined, bleached, and deodorized palm oil; $RBDPO_{SO}$, refined, bleached, and deodorized palm superolein; RPO_O, red palm olein; $RBDPO_S$, refined, bleached, and deodorized palm stearin; CtO, coconut oil; PKO, palm kernel oil; CnO, corn oil; PtO, peanut oil.

TABLE 2
Fatty Acid Composition (area %) and Iodine Value (g of I_2/100 g oil) of Edible Oil Samples[a]

Fatty acid (area %)	Sample								
	SaO	SeO	SoO	SuO	HtO	WtO	GsO	CaO	OeO
6:0	—	—	—	—	—	—	—	—	—
8:0	—	—	—	—	—	—	—	—	—
10:0	—	—	—	—	—	—	—	—	—
12:0	—	—	—	—	—	—	—	—	—
14:0	—	—	—	—	—	—	—	—	—
16:0	7.8 ± 0.0	13.0 ± 0.1	12.6 ± 0.1	8.1 ± 0.2	6.4 ± 0.2	8.7 ± 0.1	8.5 ± 0.2	5.6 ± 0.2	14.0 ± 0.5
16:1	—	—	—	—	—	—	—	—	1.2 ± 0.1
18:0	2.6 ± 0.0	6.1 ± 0.0	4.3 ± 0.0	4.8 ± 0.0	2.1 ± 0.0	2.7 ± 0.1	4.0 ± 0.1	2.5 ± 0.1	2.8 ± 0.0
18:1	13.9 ± 0.2	40.6 ± 0.1	23.6 ± 0.1	17.8 ± 0.0	74.9 ± 0.2	17.8 ± 0.1	18.4 ± 0.1	61.8 ± 0.2	72.5 ± 0.5
18:2	75.7 ± 0.1	40.3 ± 0.1	53.3 ± 0.1	69.4 ± 0.2	16.9 ± 0.1	59.0 ± 0.0	69.1 ± 0.4	20.0 ± 0.4	8.4 ± 0.0
18:3	—	—	6.3 ± 0.0	—	—	11.7 ± 0.1	—	8.1 ± 0.2	0.7 ± 0.0
20:0	—	—	—	—	—	—	—	0.8 ± 0.0	0.4 ± 0.0
20:1	—	—	—	—	—	—	—	1.3 ± 0.1	—
22:0	—	—	—	—	—	—	—	—	—
Iodine value	145.38 ± 0.46	109.24 ± 0.23	135.70 ± 0.19	139.95 ± 0.71	95.57 ± 0.57	143.28 ± 0.57	140.58 ± 0.65	107.84 ± 0.09	86.38 ± 0.11

[a]Each value in the table represents the means ± SD of triplicate analyses. Abbreviations: SaO, safflower oil; SeO, sesame oil; SoO soybean oil; SuO, sunflower oil; HtO, hazelnut oil; WtO, walnut oil; GsO, grapeseed oil; CaO, canola oil; OeO, olive oil.

TABLE 3
Distribution of Saturated, Monounsaturated, and Polyunsaturated Fatty Acids in Edible Oil Samples[a]

Sample	Fatty acid distribution (%)		
	SFA	MUFA	PUFA
Group 1			
RBDPO	54.7 ± 0.3^{d}	37.1 ± 0.2^{h}	8.1 ± 0.1^{m}
$RBDPO_{SO}$	47.6 ± 0.4^{e}	42.0 ± 0.3^{f}	10.4 ± 0.1^{k}
RPO_{O}	43.8 ± 1.4^{e}	44.2 ± 1.1^{e}	12.0 ± 0.3^{j}
$RBDPO_{S}$	74.8 ± 0.8^{c}	20.6 ± 0.6^{k}	4.6 ± 0.2^{n}
CtO	96.0 ± 0.4^{a}	3.3 ± 0.2^{o}	0.7 ± 0.2^{p}
PKO	89.7 ± 0.3^{b}	8.9 ± 0.3^{n}	1.5 ± 0.0^{o}
Group 2			
CnO	15.9 ± 0.1^{h}	27.5 ± 0.2^{i}	56.7 ± 0.4^{e}
PtO	22.5 ± 0.8^{f}	50.1 ± 0.2^{d}	27.4 ± 0.6^{h}
SaO	10.4 ± 0.0^{h}	13.9 ± 0.2^{m}	75.7 ± 0.1^{a}
SeO	19.1 ± 0.1^{f,g}	40.6 ± 0.1^{g}	40.3 ± 0.1^{f}
SoO	16.9 ± 0.1^{g}	23.6 ± 0.1^{j}	59.5 ± 0.1^{d}
SuO	12.8 ± 0.8^{h}	17.8 ± 0.0^{l}	69.4 ± 0.2^{c}
Group 3			
HtO	8.5 ± 0.1^{h}	74.9 ± 0.2^{a}	16.6 ± 0.1^{i}
WtO	11.4 ± 0.0^{h}	17.8 ± 0.1^{l}	70.7 ± 0.1^{b}
GsO	12.5 ± 0.2^{h}	18.4 ± 0.1^{l}	69.1 ± 0.4^{c}
CaO	8.9 ± 0.1^{h}	63.1 ± 0.1^{c}	28.1 ± 0.2^{g}
OeO	17.2 ± 0.5^{g}	73.7 ± 0.5^{b}	9.1 ± 0.0^{l}

[a]Each value in the table represents the means ± SD of triplicate analyses. Means within each column with different superscripts are significantly ($P < 0.01$) different. Abbreviations: SFA, saturated fatty acid; MUFA, monounsaturated fatty acid; PUFA, polyunsaturated fatty acid. For other abbreviations see Tables 1 and 2.

were derived from the same plant origin, they differ considerably in their characteristics and properties. PKO was similar to CtO in that they were both high in lauric ($C_{12:0}$) and myristic ($C_{14:0}$) acids. Nevertheless, PKO had a lower content of short-chain FA ($C_{6:0}$–$C_{10:0}$) and a slightly higher oleic ($C_{18:1}$) acid content. These slight differences were reflected in a higher IV for PKO. In CtO, the SFA content was significantly ($P < 0.01$) higher, while MUFA and PUFA contents were significantly ($P < 0.01$) lower than all edible oils and fats used in this study.

Oil samples in Group 2 were characterized by their high IV levels (95–145 g of I_2/100 g oil). The unsaturated FA (MUFA and PUFA) made up about 78–90%, while SFA formed the remaining 10–22% of total FA. The oils were primarily composed of four major FA, namely $C_{16:0}$, $C_{18:0}$, $C_{18:1}$, and linoleic ($C_{18:2}$) acid. A substantial amount of linolenic ($C_{18:3}$) acid was found in soybean oil (SoO) and corn oil (CnO) at concentrations of 6.3 and 0.9%, respectively. In addition to the four major FA mentioned earlier, peanut oil (PtO) was also composed of other minor FA: arachidic ($C_{20:0}$), gadoleic ($C_{20:1}$), and behedic ($C_{22:0}$) acids. Safflower oil (SaO) and sunflower oil (SuO) were characterized by their high concentrations of $C_{18:2}$; 75.7 and 69.4%, respectively.

Oil samples in Group 3 were also characterized by their high IV levels (86–143 g of I_2/100 g oil). The unsaturated FA (MUFA and PUFA) made up about 83–92%, while SFA formed the remaining 8–17% of total FA. Hazelnut oil (HtO), canola oil (CaO), and olive oil (OeO) were largely made up of $C_{18:1}$; 74.9, 63.1, and 72.5%, respectively. Walnut oil (WtO) and grapeseed oil (GsO) showed comparable FA composition, except that WtO contained a marked amount of $C_{18:3}$ (11.7 %).

TABLE 4
Triacylglycerol Composition (area %) of Edible Oil Samples from Group 1[a]

	Sample (Group 1)					
TAG	RBDPO	$RBDPO_{SO}$	RPO_{O}	$RBDPO_{S}$	CtO	PKO
CCLa					12.9 ± 0.2	6.8 ± 0.0
CLaLa					17.4 ± 0.2	9.9 ± 0.0
LaLaLa					21.2 ± 0.3	21.2 ± 0.2
LaLaM					18.0 ± 0.3	17.0 ± 0.0
LaLaO					3.1 ± 0.0	5.3 ± 0.0
LaMM					10.2 ± 0.1	8.8 ± 0.0
MMM	0.4 ± 0.0	0.7 ± 0.0	0.6 ± 0.0	0.2 ± 0.0		
LaLaP					0.5 ± 0.0	1.2 ± 0.0
LaMO					2.4 ± 0.1	4.6 ± 0.0
MPL	2.4 ± 0.1	3.2 ± 0.0	3.7 ± 0.1	1.0 ± 0.2		
LaMP					5.5 ± 0.1	4.6 ± 0.0
LaOO					1.1 ± 0.0	3.8 ± 0.0
LaPO					1.6 ± 0.2	4.3 ± 0.0
LaPP + MMO				2.1 ± 0.3	1.9 ± 0.0	
OOL	0.7 ± 0.0	0.7 ± 0.0	0.8 ± 0.1	0.1 ± 0.0		
MMP	1.8 ± 0.1	2.3 ± 0.1	2.6 ± 0.1	0.8 ± 0.1	0.2 ± 0.0	0.7 ± 0.1
MOO					0.8 ± 0.1	2.0 ± 0.0
MPO + POL				1.1 ± 0.0	2.1 ± 0.0	
POL	10.1 ± 0.0	12.8 ± 0.0	15.8 ± 0.1	5.3 ± 0.5		
PPL	9.8 ± 0.1	10.7 ± 0.0	11.2 ± 0.0	7.8 ± 0.0		0.6 ± 0.1
MPP	0.6 ± 0.0			2.3 ± 0.0		
OOO	4.1 ± 0.0	4.9 ± 0.0	5.6 ± 0.0	1.8 ± 0.0	0.6 ± 0.1	1.4 ± 0.0
POO	24.2 ± 0.1	29.1 ± 0.1	36.3 ± 0.0	12.0 ± 0.2	0.3 ± 0.0	1.9 ± 0.1
PPO	31.1 ± 0.1	27.2 ± 0.1	17.1 ± 0.1	29.8 ± 0.0	0.7 ± 0.1	1.1 ± 0.1
PPP	5.9 ± 0.0		0.1 ± 0.0	29.2 ± 0.2	0.6 ± 0.1	0.1 ± 0.0
SOO	2.3 ± 0.1	3.1 ± 0.1	3.6 ± 0.0	0.8 ± 0.1		0.4 ± 0.1
PSO	5.1 ± 0.0	5.0 ± 0.1	2.5 ± 0.1	3.8 ± 0.0		0.4 ± 0.1
PPS	0.9 ± 0.0			5.2 ± 0.2		
SSO	0.5 ± 0.0	0.4 ± 0.1				

[a]Each value in the table represents the means ± SD of triplicate analyses. Abbreviations: TAG, triacylglycerol; C, capric; La, lauric; M, myristic; P, palmitic; S, stearic; O, oleic; L, linoleic. For other abbreviations see Table 1.

TAG compositional and proportional analyses. The degree of unsaturation has the greatest effect on separation. The presence of double bonds in a TAG decreases its retention time on the column. About 55 different TAG have been found in the oil samples used in this study (Tables 4–6). The minor or major TAG were not similar in these oil samples, and a general analogy for the identical TAG was not easily achieved. Furthermore, a complete range of the necessary standard TAG was not available for calibration purposes. Therefore, some TAG peak identification was done according to the previously studied results (6,9, 29–32). From the results obtained by HPLC analysis, TAG could be further divided into four component categories: the first one corresponds to trisaturated (SSS) TAG; the second to disaturated–monounsaturated (SSU) TAG; the third to monosaturated–diunsaturated (SUU) TAG; and the fourth corresponds to triunsaturated (UUU). The TAG are grouped according to these categories for each type of oil sample in Table 7. The arrays of SSS, SSU, SUU, and UUU means of the oil and fat samples were further evaluated by the Duncan's multiple-range test (Table 7).

The TAG composition of the six oil samples in Group 1 (Table 4) agree with previously reported findings. Note that in palm-based oil samples (RBDPO, $RBDPO_{SO}$, RPO_{O}, and $RBDPO_{S}$), POO and PPO (P, palmitic; O, oleic) account for up to 56% of the TAG. Besides POO and PPO, $RBDPO_{SO}$ also predominantly contained PPP (29.2%), a completely saturated TAG. Thus, in $RBDPO_{SO}$, SSS, and SSU constituted more than 75% of total TAG. On the other hand, RBDPO, $RBDPO_{SO}$, and RPO_{O}, mainly consisted of SSU (34–48%) and SUU (36–55%), with small quantities of SSS (3–10%) and UUU (4–7%). PKO and CtO are characterized as hard oils. There were many similarities between PKO and CtO in terms of their TAG compositions. The saturated TAG (SSS) were the major TAG of PKO and CtO and accounted for 70 and 86%, respectively, of the total TAG. Of these, LaLaLa and LaLaM (La, lauric; M, myristic) were the major SSS TAG.

The oils in Group 2 generally contained a high level of UUU (> 54%). Their specific TAG composition in Table 5 confirms that $C_{16:0}$, $C_{18:1}$, and $C_{18:2}$ accounted for over 90% of the FA in these oils. The predominant type of TAG in CnO, SaO, SoO, and SuO was LLL (L, linoleic), which accounted for 23.6, 48.9, 20.8, and 35.0%, respectively, of all TAG. In PtO and sesame oil (SeO), the predominant TAG were OOL (21.1%) and OLL (19.7%), respectively.

The five oil samples in Group 3 also contained a high level of UUU (>60%). Among the TAG, LLL was the predominant TAG in WtO and GsO and accounted for 25.7 and 38.7%, re-

TABLE 5
Triacylglycerol Composition (area %) of Edible Oil Samples from Group 2[a]

	Sample (Group 2)					
TAG	CnO	PtO	SaO	SeO	SoO	SuO
LLnLn			1.5 ± 0.3	0.3 ± 0.1	2.0 ± 0.3	
LLLn	1.7 ± 0.1	1.0 ± 0.2	1.2 ± 0.4	0.6 ± 0.0	9.3 ± 0.1	0.4 ± 0.0
OLnLn					0.6 ± 0.0	
LLL	23.6 ± 0.1	3.6 ± 0.1	48.9 ± 0.1	10.7 ± 0.0	20.8 ± 0.6	35.0 ± 0.0
OLLn	0.7 ± 0.0				1.2 ± 0.1	
PLLn					3.7 ± 0.0	
OLL	22.2 ± 0.3	12.5 ± 0.3	17.7 ± 0.1	19.7 ± 0.1	16.0 ± 0.3	25.3 ± 0.1
PLL	14.6 ± 0.2	4.5 ± 0.0	13.7 ± 0.0	7.4 ± 0.0	14.1 ± 0.4	11.1 ± 0.1
POLn					0.4 ± 0.0	
OOL	10.9 ± 0.1	20.0 ± 0.6	4.0 ± 0.1	17.9 ± 0.1	7.6 ± 0.1	6.3 ± 0.0
POL + SLL	11.4 ± 0.1		8.0 ± 0.1	14.2 ± 0.1	11.2 ± 0.0	12.6 ± 0.1
POL		12.6 ± 0.3				
PPL	2.0 ± 0.0	1.9 ± 0.0	0.6 ± 0.0	1.5 ± 0.1	1.9 ± 0.1	0.9 ± 0.0
OOO	4.3 ± 0.0	17.4 ± 0.0	1.7 ± 0.2	9.0 ± 0.2	2.3 ± 0.2	1.7± 0.1
POO + SOL	5.8 ± 0.1	12.7 ± 0.9	2.3 ± 0.1	12.1 ± 0.1	5.0 ± 0.5	3.6 ± 0.1
PPO	2.4 ± 0.0	2.5 ± 0.1	0.4 ± 0.1	2.3 ± 0.3	2.0 ± 0.0	1.3 ± 0.1
PPP		0.5 ± 0.0				
SLL						1.1 ± 0.1
PSL		1.5 ± 0.1				
SOO + PSO		4.4 ± 0.2				
SOO	0.4 ± 0.0			3.3 ± 0.1	1.0 ± 0.1	0.5 ± 0.0
PSO	0.2 ± 0.0			1.0 ± 0.1	0.9 ± 0.0	0.1 ± 0.0
OLA		0.2 ± 0.0				
PLB		0.2 ± 0.0				
OOA		1.0 ± 0.1				
POB		0.4 ± 0.1				
OOB		2.4 ± 0.7				
OOLi		0.9 ± 0.1				

[a]Each value in the table represents the mean ± standard deviation of triplicate analyses. Abbreviations: Ln, linolenic; A, arachidic; B, behenic; Li, lignoceric. For other abbreviations see Tables 1, 2, and 4.

TABLE 6
Triacylglycerol Composition (area %) of Edible Oil Samples from Group 3[a]

	Sample (Group 3)				
TAG	HtO	WtO	GsO	CaO	OeO
LLnLn		4.2 ± 0.1		1.2 ± 0.5	
LLLn	0.5 ± 0.2	15.4 ± 0.0	0.8 ± 0.2	2.6 ± 0.6	
OlnLn		0.8 ± 0.0		1.6 ± 0.3	
LLL	2.9 ± 0.0	25.7 ± 0.0	38.7 ± 0.1	8.5 ± 0.0	0.5 ± 0.0
OLLn		3.2 ± 0.0			0.2 ± 0.0
PLLn		5.0 ± 0.0	0.1 ± 0.0	0.8 ± 0.0	
OLL	7.5 ± 0.1	14.5 ± 0.0	22.3 ± 0.1	7.5 ± 0.1	2.8 ± 0.7
OOLn				8.9 ± 0.2	1.8 ± 0.4
PLL	1.3 ± 0.0	13.0 ± 0.0	13.7 ± 0.1	1.0 ± 0.0	0.3 ± 0.2
POLn				0.2 ± 0.0	
OOL	20.2 ± 0.1	5.5 ± 0.0	6.1 ± 0.1	21.8 ± 0.2	13.0 ±0.1
POL + SLL	3.9 ± 0.2	7.3 ± 0.0	12.3 ± 0.1	5.5 ± 0.0	
POL					6.4 ± 0.1
PPoL					0.9 ± 0.0
PPL	0.3 ± 0.1	0.5 ± 0.0	0.1 ± 0.0		
PSLn				0.4 ± 0.0	
OOO	48.6 ± 0.4	2.1 ± 0.0	1.9 ± 0.1	28.3 ± 0.2	41.8 ± 0.2
POO + SOL	10.3 ± 0.5	2.2 ± 0.1	3.9 ± 0.1	6.8 ± 0.0	21.9 ± 0.2
PPO	0.5 ± 0.0	0.4 ± 0.0	0.1 ± 0.0	0.9 ± 0.1	3.0 ± 0.1
PPP	0.1 ± 0.0				
OOGa				1.0 ± 0.2	0.6 ± 0.0
SOO	3.8 ± 0.1	0.2 ± 0.0	0.4 ± 0.0	3.1 ± 0.2	4.9 ± 0.2
PSO	0.3 ± 0.0				1.0 ± 0.1
OOA					0.5 ± 0.0
SSO					0.3 ± 0.0

[a]Each value in the table represents the means ± SD of triplicate analyses. Abbreviations: Po, palmitoleic; Ga, gadoleic. For other abbreviations see Tables 2, 4, and 5.

TABLE 7
Distribution of Trisaturated, Monounsaturated, Diunsaturated, and Triunsaturated Triacylglycerols (TAG) in Edible Oil Samples[a]

Sample	TAG distribution (%)			
	SSS	SSU	SUU	UUU
Group 1				
RBDPO	9.8 ± 0.1[d]	48.8 ± 0.1[a]	36.5 ± 0.2[c]	4.8 ± 0.0[k]
RBDPOSO	2.9 ± 0.1[e]	46.5 ± 0.1[b]	44.9 ± 0.1[b]	5.6 ± 0.0[j,k]
RPOO	3.3 ± 0.1[e]	34.6 ± 0.0[d]	55.7 ± 0.1[a]	6.4 ± 0.1[j]
RBDPOS	37.7 ± 0.1[c]	42.3 ± 0.2[c]	18.1 ± 0.6[l]	1.9 ± 0.0[l]
CtO	86.4 ± 0.7[a]	6.1 ± 0.1[g]	1.3 ± 0.1[n]	0.6 ± 0.1[m]
PKO	70.3 ± 0.1[b]	16.3 ± 0.1[e]	6.0 ± 0.1[m]	1.4 ± 0.0[l,m]
Group 2				
CnO	—	4.5 ± 0.0[i,j]	32.1 ± 0.3[f]	63.4 ± 0.3[f]
PtO	0.5 ± 0.0[f]	6.5 ± 0.0[f]	34.2 ± 1.3[e]	54.5 ± 1.2[i]
SaO	—	1.0 ± 0.0[m]	24.0 ± 0.2[j]	75.0 ± 0.2[c]
SeO	—	4.8 ± 0.1[h]	37.0 ± 0.1[c]	58.2 ± 0.1[h]
SoO	—	4.8 ± 0.1[h,i]	35.4 ± 1.0[d]	59.8 ± 1.1[g]
SuO	—	2.3 ± 0.1[k]	28.9 ± 0.1[h]	68.8 ± 0.2[e]
Group 3				
HtO	0.1 ± 0.0[g]	1.0 ± 0.1[m]	19.2 ± 0.6[k]	79.6 ± 0.8[b]
WtO	—	0.9 ± 0.0[m]	27.7 ± 0.1[i]	71.4 ± 0.0[d]
GsO	—	0.1 ± 0.0[n]	30.3 ± 0.1[g]	69.7 ± 0.1[e]
CaO	—	1.3 ± 0.2[l]	17.4 ± 0.2[l]	81.3 ± 0.1[a]
OeO	—	4.4 ± 0.2[j]	35.0 ± 0.3[d,e]	60.7 ± 0.1[g]

[a]Each value in the table represents the means ± SD of triplicate analyses. Means within each column with different superscripts are significantly ±$P < 0.01$) different. Abbreviations: S represents saturated fatty acids; U represents unsaturated fatty acids; SSS, trisaturated triacylglycerol; SSU, monounsaturated triacylglycerol; SUU, diunsaturated; UUU, triunsaturated triacylglycerol. The sequence does not necessarily reveal their position on the glycerine moiety. For other abbreviations, see Tables 1 and 2.

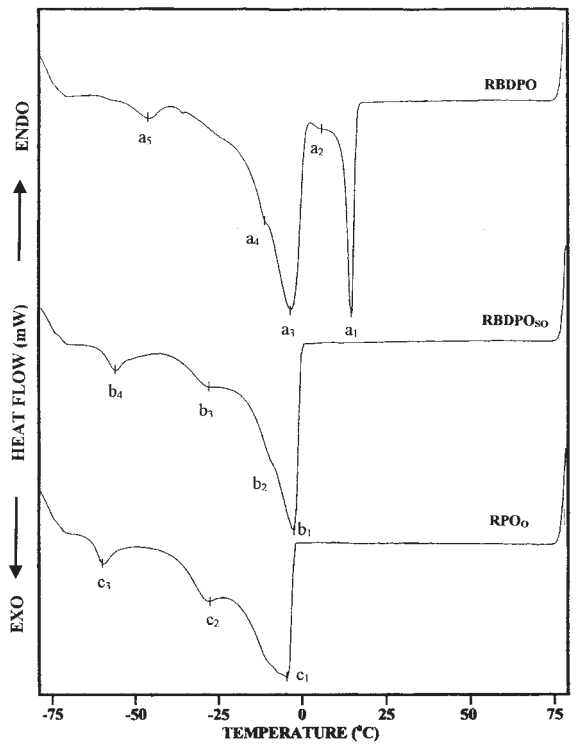

FIG. 1. Differential scanning calorimetry crystallization curves of refined-bleached-deodorized palm oil (RBDPO), refined-bleached-deodorized palm superolein ($RBDPO_{SO}$), and red palm olein (RPO_O). Refer to Table 8 for transition temperatures.

spectively. Conversely, OOO was the predominant TAG in HtO, CaO and OeO, which accounted for 48.6, 28.3, and 41.8%, respectively, of all TAG.

Thermal analysis. Melting and crystallization, two commonly used physical events to characterize thermal behavior of oil samples, require the intake or release of thermal enthalpy. DSC is eminently suitable to determine these physical properties of oil samples. Thermal curves, as determined by DSC, are given in Figures 1–8. Crystallization curves of oil samples are illustrated in Figures 1–4, while the melting curves are displayed in Figures 5–8. Generally, in melting curves of oil samples, complex features that were not easily interpretable, such as shoulders not separable from peaks, were noticed. These results illustrate the complex nature of TAG in oil samples. This is a consequence of the known phenomenon of polymorphism of natural oils and fats that has interested researchers for many years. Unlike pure TAG, the polymorphic form of oils and fats cannot be established unequivocally by DSC (35). This can only be achieved by X-ray diffraction analysis. Therefore, polymorphic transformations in oil samples have not been reported in this study. Due to the complexity of the recorded thermal events, all melting and crystallization points are read at the maximum/minimum of either endo- or exotherm peaks. Overall, the designation of these transition temperatures for melting and crystallization curves are clearly indicated in Tables 8, 9, and 10, for oil samples in Groups 1, 2, and 3, respectively.

The crystallization curves of six oil samples in Group 1 are illustrated in Figures 1 (RBDPO, $RBDPO_{SO}$, and RPO_O) and 2 ($RBDPO_S$, CtO, and PKO). In RBDPO, the crystallization curve

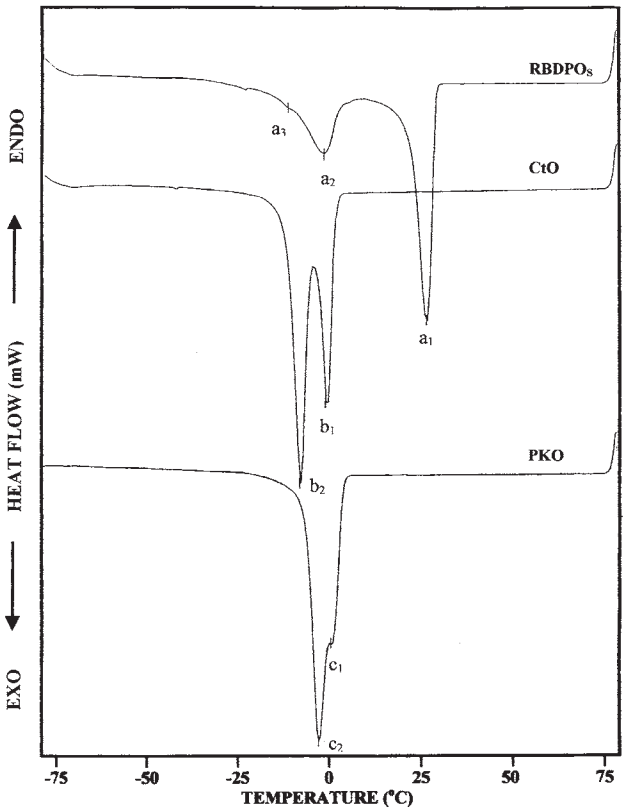

FIG. 2. Differential scanning calorimetry crystallization curves of refined-bleached-deodorized palm stearin ($RBDPO_S$), coconut oil (CtO), and palm kernel oil (PKO). Refer to Table 8 for transition temperatures.

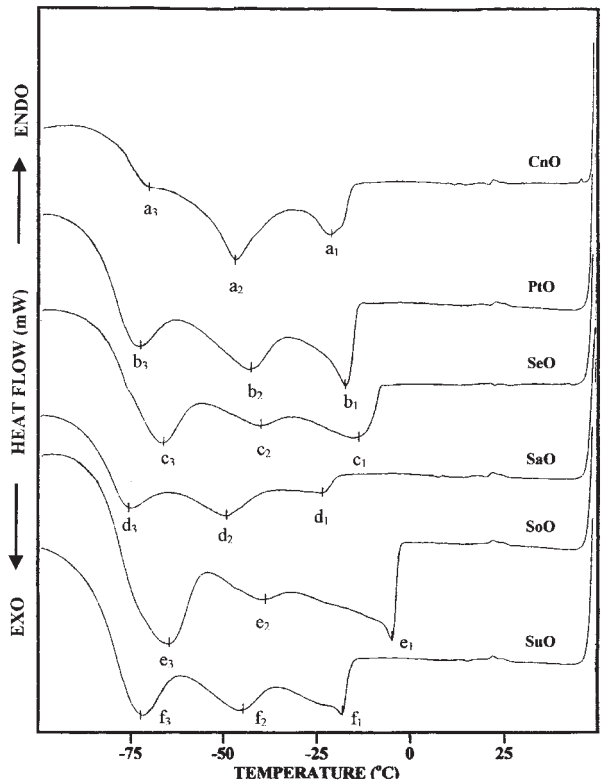

FIG. 3. Differential scanning calorimetry crystallization curves of corn oil (CnO), peanut oil (PtO), sesame oil (SeO), safflower oil (SaO), soybean oil (SoO), and sunflower oil (SuO). Refer to Table 9 for transition temperatures.

displayed two major exothermic regions. The higher temperature region defined crystallization of the stearin fraction, while the lower temperature region indicated crystallization of the olein fraction (Fig. 1). Figure 1 shows that the higher temperature region was absent in the crystallization curves of $RBDPO_{SO}$, and RPO_O. The crystallization curve of $RBDPO_S$ had both regions, although the higher temperature region in $RBDPO_S$ was apparently the major feature (Fig. 2). The crystallization curve of CtO showed two distinct exothermic peaks, whereas PKO showed two overlapping exothermic peaks (Fig. 2).

Figure 3 shows DSC crystallization curves for the oil samples in Group 2. All curves have three distinct exothermic peaks (high, medium, and low-temperature peaks, respectively), which may correspond to three major TAG groups (SSU, SUU, and UUU, respectively). Of all oil samples in this group, the three transition temperatures of the SaO peaks were consistently the lowest. This could be due to its significantly ($P < 0.01$) higher content of UUU than to the five other oil samples in Group 2 (Table 7).

DSC crystallization curves of oil samples in Group 3 (Figure 7) also exhibit three exotherm peaks, except for HtO. HtO showed a distinct tall exotherm peak at –49.84°C and a small shoulder peak at –27.57°C (Table 9). This is most likely due to its high content of OOO. In general, the lowest exotherm peaks (last crystallizing) for WtO, GsO, CaO, and OeO were sharper and taller than the two smaller exotherm peaks. Moreover, the two exotherm peaks at higher temperatures in OeO and CaO were not as apparent as those of WtO and GsO. Again, this could be due to the high OOO content in OeO and CaO.

The DSC melting curves of the oil samples in Group 1 are presented in Figures 5 ($RBDPO$, $RBDPO_{SO}$, and RPO_O) and 6 ($RBDPO_S$, CtO, and PKO). The melting curve of RBDPO showed two major endotherm regions (Fig. 5), corresponding to endothermic transitions of the olein (lower-temperature peak) and stearin (higher-temperature peak) fractions. The endotherm region at higher temperature consisted of a plateau with a pair of shoulder peaks, while the endotherm region at lower temperature contained four overlapping peaks. However, $RBDPO_{SO}$ and RPO_O showed only one major endotherm in the lower temperature region (olein fraction), and both oil samples had typical melting curves. $RBDPO_S$ showed both endotherm regions (Fig. 6); the higher region was distinguished by a tall peak (and two small fusion peaks) preceding the low region (consisting of four small merging peaks). The small low-temperature peak in the melting curve of $RBDPO_S$ indicated that a small amount of olein was trapped in this oil sample after fractionation. These results agree with our earlier observation from the crystallization curves. In CtO, a major endothermic peak with a shoulder peak and a small distinct endothermic peak were observed (Fig. 6), while a major endotherm peak with a shoulder peak and two small fusion peaks were noticed in PKO (Fig. 6).

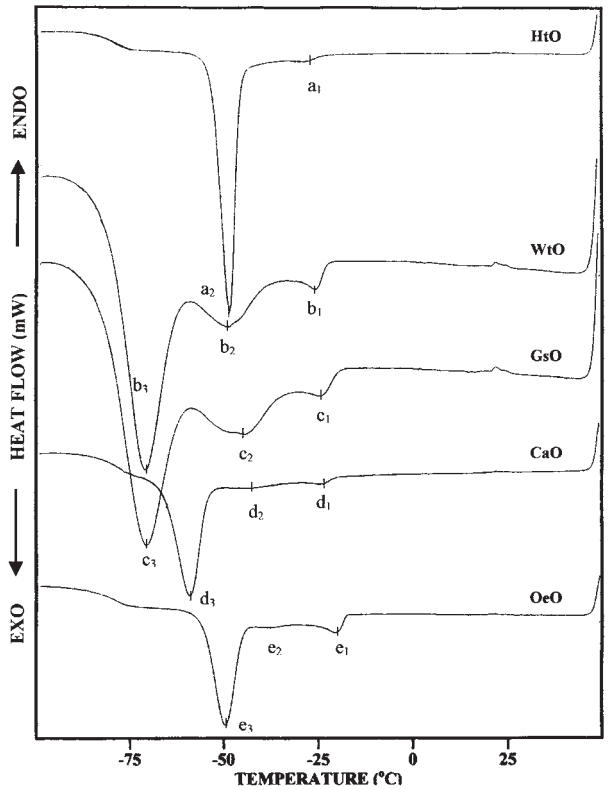

FIG. 4. Differential scanning calorimetry crystallization curves of hazelnut oil (HtO), walnut oil (WtO), grapeseed oil (GsO), canola oil (CaO), and olive oil (OeO). Refer to Table 10 for transition temperatures.

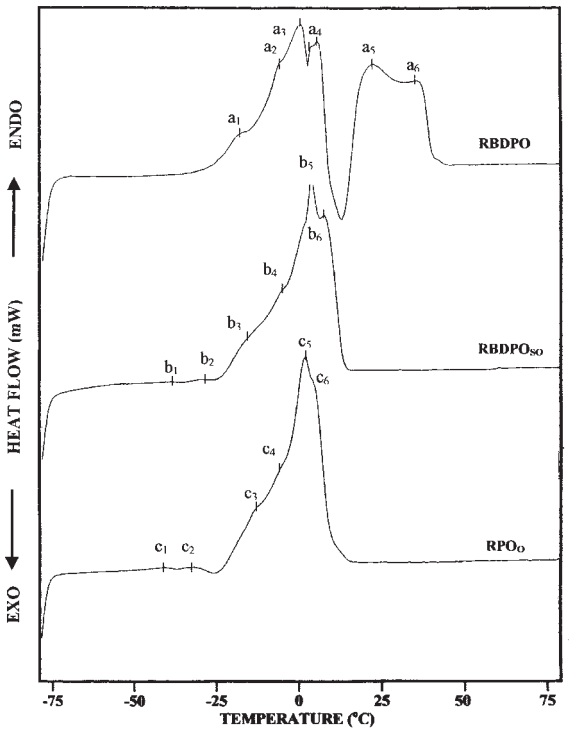

FIG. 5. Differential scanning calorimetry melting curves of RBDPO, RBDPO$_{SO}$, and RPO$_O$. See Figure 1 for abbreviations. Refer to Table 8 for transition temperatures.

Figure 7 shows the DSC melting curves of oil samples in Group 2. Overall, all samples showed two distinct endotherm regions, the higher temperature feature (later melting) being the major one, except for SuO. In CnO, PtO, SeO, and SoO, the major endotherm region at higher temperatures had a distinct high peak and a plateau of one or two shoulder peak(s) (Fig. 7). The melting curve for SuO consisted of four peaks. The first and last peaks were the major features with two small merging peaks in between.

Figure 8 compares the typical DSC melting curves of oil samples in Group 3. The melting curve of HtO consisted of a single tall endotherm peak at –9.07°C, whereas four other types of oil (WtO, GsO, CaO, and OeO) showed a distinct tall endotherm peak with some merging small shoulder peaks (Fig. 8).

Generally speaking, the thermal properties of various oil samples from the DSC melting and crystallization curves can be characterized by various transition temperatures. Nevertheless, comparison of these transition temperatures is evidently difficult because of their complex features. Therefore, a more systematic and convenient way to differentiate edible oils and fats has been carried out in this study. Three DSC parameters, namely T_o, T_f, temperature range (difference between T_o and T_f), were established for each thermal curve in all oil samples. A complete comparison of these three DSC parameters is summarized in Tables 11 and 12 for crystallization and melting curves, respectively. Data for these parameters were analyzed

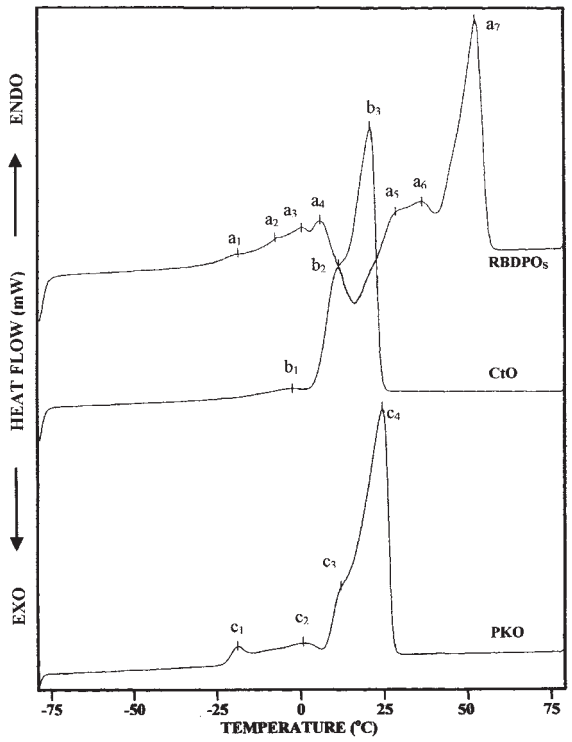

FIG. 6. Differential scanning calorimetry melting curves of RBDPO$_S$, coconut oil (CtO), and palm kernel oil (PKO). See Figure 2 for abbreviations. Refer to Table 8 for transition temperatures.

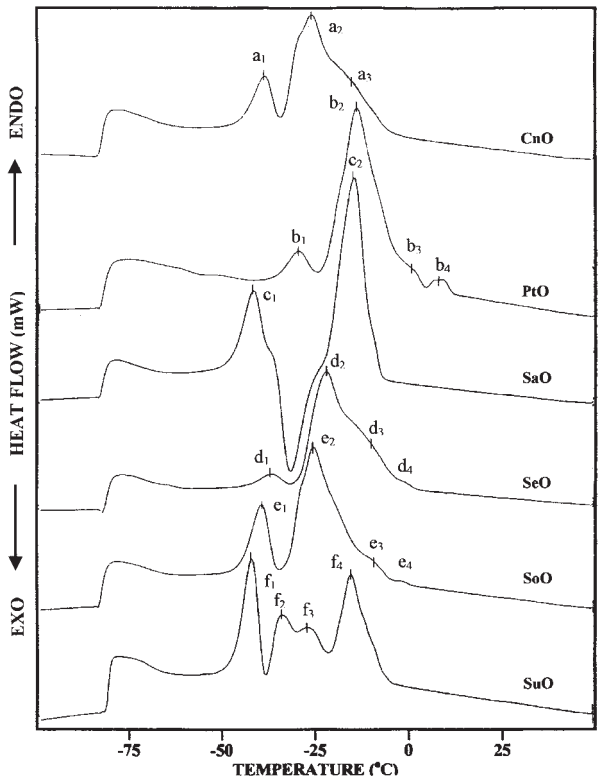

FIG. 7. Differential scanning calorimetry melting curves of CnO, PtO, SaO, SeO, SoO, and SuO. See Figure 3 for abbreviations. Refer to Table 9 for transition temperatures.

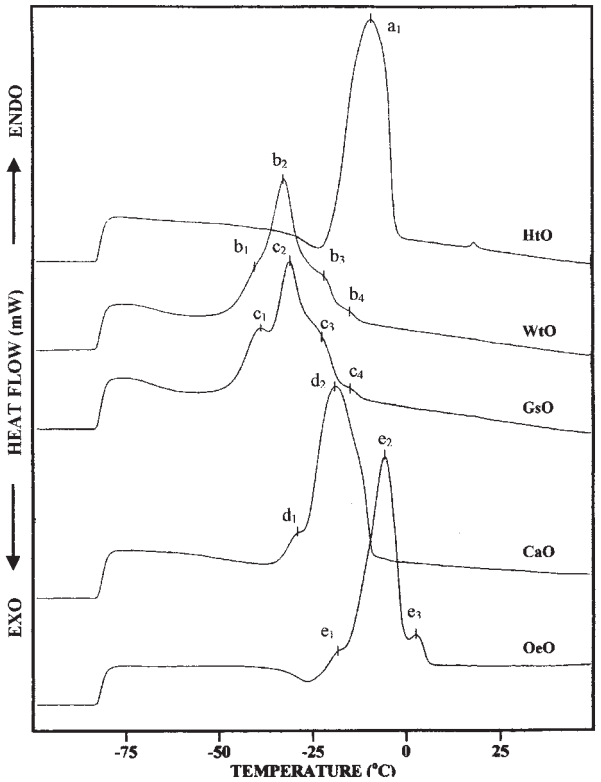

FIG. 8. Differential scanning calorimetry melting curves of HtO, WtO, GsO, CaO, and OeO. See Figure 4 for abbreviations. Refer to Table 10 for transition temperatures.

by utilizing conventional statistical methods and tests of significance (Duncan's multiple-range test). Obviously, comparison among these parameters showed significant ($P < 0.01$) differences between T_o for the crystallization curves and T_f for the melting curves. Generally, T_o for the crystallization curves of the oils in Group 1 showed significantly ($P < 0.01$) higher values than the oil samples in Groups 2 and 3. However, T_f for the melting curves of the oil samples in Groups 2 and 3 were

TABLE 8
Comparison of Differential Scanning Calorimetry-Measured Transition Temperatures for Melting and Crystallization Curves of Edible Oil Samples in Group 1[a]

		Transition temperature (°C)[b]						
Curve	Sample	1	2	3	4	5	6	7
Crystallization	RBDPO	15.43	6.11	–2.85	–11.09	–46.92		
	$RBDPO_{SO}$	–2.85	–8.94	–28.29	–56.95			
	RPO_O	–3.92	–27.57	–60.54				
	$RBDPO_S$	27.25	–1.41	–11.09				
	CtO	–0.70	–7.86					
	PKO	–1.09	–2.49					
Melting	RBDPO	–18.40	–6.22	0.23	5.25	21.91	35.35	
	$RBDPO_{SO}$	–38.47	–28.43	–15.53	–4.78	3.82	8.12	
	RPO_O	–41.33	–32.73	–12.67	–5.50	2.38	4.18	
	$RBDPO_S$	–18.40	–6.93	0.95	6.68	29.62	37.50	55.06
	CtO	–2.64	12.42	22.45				
	PKO	–19.12	1.31	13.13	26.03			

[a]Each value in the table represents the means for four determinations. SD of the reported results are in the range of 0–0.51°C and 0–1.01°C for the crystallization and melting curves, respectively.
[b]Based on indicators a, b, and c in Figures 4 and 5 for cooling curves and Figures 8 and 9 for heating curves. Abbreviations: see Table 1.

TABLE 9
Comparison of Differential Scanning Calorimetry-Measured Transition Temperatures for Melting and Crystallization Curves of Edible Oil Samples in Group 2[a]

		Transition temperature (°C)[b]				
Curve	Sample	1	2	3	4	5
Crystallization	CnO	–18.49	–44.62	–71.84		
	PtO	–5.02	–38.84	–65.24		
	SaO	–22.89	–48.74	–75.42		
	SeO	–14.09	–39.94	–66.62		
	SoO	–19.49	–43.24	–73.77		
	SuO	–19.87	–45.99	–72.12		
Melting	CnO	–39.32	–26.67	–14.85		
	PtO	–51.70	–29.70	–14.57	0.83	8.26
	SaO	–41.80	–14.30			
	SeO	–37.12	–21.45	–9.62	–0.82	
	SoO	–39.60	–25.57	–9.90	–2.47	
	SuO	–41.25	–32.82	–26.12	–14.30	

[a]Each value in the table represents the means for four determinations. SD of the reported results are in the range of 0–1.94°C and 0–1.56°C for the crystallization and melting curves, respectively.
[b]Based on indicators a, b, c, d, and e in Figure 6 for cooling curves and Figure 10 for heating curves. Abbreviations: see Tables 1 and 2.

TABLE 10
Comparison of Differential Scanning Calorimetry-Measured Transition Temperatures for Melting and Crystallization Curves of Edible Oil Samples in Group 3[a]

		Transition temperature (°C)[b]			
Curve	Sample	1	2	3	4
Crystallization	HtO	–27.57	–49.84		
	WtO	–25.92	–48.47	–70.19	
	GsO	–23.72	–44.89	–70.74	
	CaO	–23.44	–43.57	–60.02	
	OeO	–19.59	–49.29		
Heating	HtO	–9.07			
	WtO	–41.52	–34.10	–22.87	–15.72
	GsO	–39.32	–31.62	–22.82	–15.12
	CaO	–29.15	–19.25		
	OeO	–18.70	–6.32	2.21	

[a]Each value in the table represents the means for four determinations. SD of the reported results are in the range of 0–0.39°C and 0–1.17°C for the crystallization and melting curves, respectively.
[b]Based on indicators a, b, c, d, e, and f in Figure 7 for cooling curves and Figure 11 for heating curves. Abbreviations: see Table 2.

significantly ($P < 0.01$) lower than the oils in Group 1. The coefficients of variation (CV) for the DSC parameters of all oil samples are presented in Tables 11 and 12 for comparison. The results reveal excellent reproducibility for determination of these DSC parameters. The oil samples were evaluated in replicates of four, and the CV was always lower than 8%.

In conclusion, DSC does not provide any direct information about the chemical composition of edible oils under a given set of experimental conditions. However, it provides useful information regarding the nature of the thermodynamic changes that are associated with the edible oils transforming from one physical state to another. These thermodynamic characteristics are sensitive to the general chemical composition of edible oils and fats and thus can be used in qualitative and quantitative ways for identification of edible oils. This study found that two DSC parameters, namely T_o for crystallization curves and T_f for melting curves, of given edible oils and fats are sensitive indicators to identify types of edible oils. One critical limitation of using DSC is the dependence of the thermal transitions on scanning rate. Regardless of which calorimeter is used, the thermal curve depends on the scanning rate, which makes it difficult, if not impracticable, to compare experiments performed at different scan rates or with different calorimeters. Nonetheless, if edible oils give rise to identical DSC scans at the same scan rate, this technique promises to offer a sensitive, rapid, and reproducible fingerprint method for quality-control purposes.

TABLE 11
Comparison of Differential Scanning Calorimetry-Measured Onset, Offset, and Range of Temperatures for Crystallization Curve of Edible Oil Samples[a]

	Temperature (°C)					
	T_o		T_f		Range[b]	
Sample	Means ± SD	CV (%)	Means ± SD	CV (%)	Means ± SD	CV (%)
Group 1						
RBDPO	17.00 ± 0.24[b]	1.42	−63.62 ± 0.03[e]	−0.04	80.62 ± 0.21[a,b]	0.27
$RBDPO_{SO}$	−0.46 ± 0.04[e]	−7.60	−62.19 ± 0.30[d]	−0.48	61.73 ± 0.26[c]	0.42
RPO_O	−1.77 ± 0.12[f]	−6.90	−64.45 ± 0.13[f]	−0.20	62.69 ± 0.25[c]	0.40
$RBDPO_S$	29.68 ± 0.14[a]	0.47	−35.99 ± 1.04[c]	−2.88	65.67 ± 0.90[d]	1.37
CtO	2.11 ± 0.02[d]	1.07	−11.78 ± 0.10[b]	−0.84	13.90 ± 0.12[e]	0.88
PKO	4.39 ± 0.36[c]	8.09	−7.32 ± 0.40[a]	−5.40	11.71 ± 0.04[e]	0.35
Group 2						
CnO	−16.20 ± 0.19[k]	−1.17	−85.71 ± 1.13[i,j,k]	−1.31	69.51 ± 1.32[a,b,c]	1.89
PtO	−2.96 ± 0.16[g]	−5.42	−85.37 ± 0.04[i,j]	−0.04	82.42 ± 0.12[a]	0.15
SaO	−19.56 ± 0.56[n]	−2.88	−89.28 ± 0.70[m]	−0.78	69.72 ± 0.13[a,b,c]	0.19
SeO	−7.23 ± 0.19[h]	−2.58	−85.78 ± 0.76[i,j,k]	−0.89	78.56 ± 0.95[a,b]	1.21
SoO	−14.13 ± 0.24[l]	−1.73	−86.76 ± 0.05[l]	−0.06	72.63 ± 0.30[a,b,c]	0.41
SuO	−15.53 ± 0.07[j]	−0.43	−86.14 ± 0.15[j,k,l]	−0.18	70.61 ± 0.22[a,b,c]	0.31
Group 3						
HtO	−23.82 ± 0.37[p]	−1.56	−85.27 ± 0.45[i]	−0.52	61.44 ± 0.82[c]	1.33
WtO	−22.63 ± 0.16[q]	−0.71	−82.55 ± 0.34[g]	−0.42	59.92 ± 0.50[c]	0.84
GsO	−18.84 ± 0.31[m]	−1.63	−83.45 ± 0.17[h]	−0.20	64.60 ± 0.14[c]	0.21
CaO	−20.33 ± 0.10[o]	−0.48	−85.74 ± 0.06[i,j,k]	−0.07	65.41 ± 0.16[c]	0.24
OeO	−17.33 ± 0.14[l]	−0.81	−86.22 ± 0.08[i,k]	−0.09	68.89 ± 0.22[b,c]	0.31

[a]Each value in the table represents the means ± SD of four determinations. Means within each column with different superscripts are significantly ($P < 0.01$) different. Abbreviations: T_o, onset temperature; T_f, offset temperature. For other abbreviations, see Tables 1 and 2.
[b]Temperature difference between T_o and T_f.

TABLE 12
Comparison of Differential Scanning Calorimetry-Measured Onset, Offset, and Range of Temperatures for Melting Curve of Edible Oil Samples[a]

	Temperature (°C)					
	T_o		T_f		Range[b]	
Sample	Means ± SD	CV (%)	Means ± SD	CV (%)	Means ± SD	CV (%)
Group 1						
RBDPO	-26.66 ± 0.61[d]	−2.28	40.59 ± 0.37[b]	0.92	67.25 ± 0.98[b]	1.46
$RBDPO_{SO}$	−46.28 ± 1.44[g]	−3.10	13.86 ± 0.21[e]	1.49	60.14 ± 1.23[c]	2.04
RPO_O	−49.95 ± 1.09[j]	−2.18	9.64 ± 0.13[g]	1.32	59.60 ± 0.96[c]	1.61
$RBDPO_S$	−28.29 ± 0.12[e]	−0.41	57.78 ± 0.53[a]	0.92	86.07 ± 0.42[a]	0.48
CtO	−21.80 ± 0.25[b]	−1.14	25.30 ± 0.01[d]	0.05	47.10 ± 0.26f	0.56
PKO	−25.56 ± 0.20[c,d]	−0.80	28.98 ± 0.00[c]	0.02	54.54 ± 0.21[d]	0.38
Group 2						
CnO	−46.02 ± 0.09[g]	−0.20	−4.21 ± 0.05[l]	−1.13	41.31 ± 0.44[g]	1.06
PtO	−56.52 ± 0.07[k]	−0.12	11.83 ± 0.03[f]	0.23	68.35 ± 0.09[b]	0.14
SaO	−48.36 ± 0.09[h,i]	−0.19	−6.64 ± 0.09[m]	1.32	41.72 ± 0.18[g]	0.43
SeO	−46.03 ± 0.96[g]	−2.09	3.36 ± 0.25[i]	7.54	49.40 ± 1.21[e]	2.46
SoO	−46.11 ± 0.06[g]	−0.13	1.89 ± 0.03[j]	1.44	47.75 ± 0.37[e,f]	0.78
SuO	−46.79 ± 0.45[g,h]	−0.97	−4.72 ± 0.06[l]	−1.35	42.57 ± 0.06[g]	0.14
Group 3						
HtO	−19.99 ± 0.22[a]	−1.11	−2.87 ± 0.12[k]	−4.34	17.11 ± 0.10[k]	0.56
WtO	−48.20 ± 0.91[h,i]	−1.89	−11.63 ± 0.42[p]	−3.58	36.57 ± 1.33[h]	3.62
GsO	−48.70 ± 0.04[i,j]	−0.08	−11.00 ± 0.10[o]	−0.94	37.70 ± 0.14[h]	0.38
CaO	−34.69 ± 0.05[f]	−0.15	−9.17 ± 0.18[n]	−1.96	25.52 ± 0.23[j]	0.90
OeO	−25.07 ± 0.00[c]	0.00	6.27 ± 0.15[h]	2.40	31.34 ± 0.15[l]	0.48

[a]Each value in the table represents the means ± SD of triplicate analyses. Means within each column with different superscripts are significantly ($P < 0.01$) different. Abbreviations: see Tables 1, 2, and 11.
[b]Temperature difference between T_o and T_f.

ACKNOWLEDGMENT

This research work was supported by Universiti Putra Malaysia (IRPA Project No. 03-02-04-003).

REFERENCES

1. Willis, W.M., R.W. Lencki, and A.G. Marangoni, Lipid Modification Strategies in the Production of Nutritionally Functional Fats and Oils, *Crit. Rev. Food Sci. Nutr. 38*:639–674 (1998).
2. Orthoefer, F.T., Vegetable Oils, in *Bailey's Industrial Oil and Fat Products*, 5th edn., edited by Y.H. Hui, John Wiley & Sons Inc., New York, 1996, Vol. 1, pp. 19–43.
3. O'Brien, R.D., Raw Materials, in *Fats and Oils: Formulating and Processing for Applications*, Technomic Publishing Company, Inc., Lancaster, PA, 1998, pp. 1–46.
4. Tsimidou, M., R. Macrae, and I. Wilson, Authentication of Virgin Olive Oils Using Principal Component Analysis of Triglyceride and Fatty Acid Profiles: Part 1-Classification of Greek Olive Oils, *Food Chem. 42*:227–239 (1987).
5. Van Niekerk, P.J., and A. Burger, The Estimation of the Composition of Edible Oil Mixtures, *J. Am. Oil Chem. Soc. 62*:531–538 (1985).
6. Dong, M.W., and J.L. Dicesare, Improved Separation of Natural Oil Triglycerides by Liquid Chromatography Using Columns Packed with 3-μm Particles, *Ibid. 60*:788–791 (1983).
7. Ruiz-Sala, P., M.T.G. Hierro, I. Martinez-Castro, and G. Santa-Maria, Triglyceride Composition of Ewe, Cow, and Goat Milk Fat, *Ibid. 73*:223–293 (1996).
8. Bornaz, Salwa, G. Novak, and M. Parmentier, Seasonal and Regional Variation in Triglyceride Composition of French Butterfat, *Ibid. 69*:1131–1135 (1992).
9. Bland, J.M., E.J. Conkerton, and G. Abraham, Triacylglyceride Composition of Cottonseed Oil by HPLC and GC, *Ibid. 68*:840–843 (1991).
10. Dollimore, D., Thermal Analysis, *Anal. Chem. 68(10)*:63R–71R (1996).
11. Biliaderis, C.G., Differential Scanning Calorimetry in Food Research—A Review, *Food Chem. 10*:239–265 (1983).
12. Cebula, D.J., and K.W. Smith, Differential Scanning Calorimetry of Confectionery Fats. Part II—Effects of Blends and Minor Components, *J. Am. Oil Chem. Soc. 69*:992–998 (1992).
13. Cebula, D.J., and K.W. Smith, Differential Scanning Calorimetry of Confectionery Fats. Pure Triglycerides: Effects of Cooling and Heating Rate Variation, *Ibid. 68*:591–595 (1991).
14. Sessa, D.J., Derivation of a Cocoa Butter Equivalent from Jojoba Transesterified Ester *via* a Differential Scanning Calorimetry Index, *J. Sci. Food Agric. 72*:295–298 (1996).
15. Rossell, J.B., Phase Diagrams of Triglyceride Systems, *Adv. Lipid Res. 5*:353–408 (1967).
16. Arishima, T., N. Sagi, H. Mori, and K. Sato, Polymorphism of POS. I. Occurrence and Polymorphic Transformation, *J. Am. Oil Chem. Soc. 68*:710–715 (1991).
17. Che Man, Y.B., and P.Z. Swe, Thermal Analysis of Failed-Batch Palm Oil by Differential Scanning Calorimetry, *Ibid. 72*:1529–1532 (1995).
18. Menard, K.P., R. Rogers, and K. Huff, Prediction of SFI Values by Differential Scanning Calorimetry [Abstract], *INFORM 5*:523 (1994).
19. Dyszel, S.M., and B.C. Pettit, Determination of the Country Origin of Pistachio Nuts by DSC and HPLC, *J. Am. Oil Chem. Soc. 67*:947–951 (1990).
20. Coni, E., M. Di Pasquale, P. Coppolelli, and A. Bocca, Detection of Animal Fats in Butter by Differential Scanning Calorimetry: A Pilot Study, *Ibid. 71*:807–810 (1994).
21. Sessa, D.J., T.C. Nelsen, R. Kleiman, and J.D. Arquette, Differential Scanning Calorimetry Index for Estimating Level of Saturation in Transesterified Wax Esters, *Ibid. 48*:271–273 (1996).
22. Haryati, T., Y.B. Che Man, A.B. Asbi, H.M. Ghazali, and L. Buana, Determination of Iodine Value of Palm Oil by Differential Scanning Calorimetry, *Ibid. 74*:939–942 (1997).
23. Tan, C.P., and Y.B. Che Man, Quantitative Differential Scanning Calorimetric Analysis for Determining Total Polar Compounds in Heated Oils, *Ibid. 76*:1047–1057 (1999).
24. Md. Ali, A.R., and P.S. Dimick, Thermal Analysis of Palm Mid-Fraction, Cocoa Butter and Milk Fat Blends by Differential Scanning Calorimetry, *Ibid. 71*:299–302 (1994).
25. Berger, K.G., and E.E. Akehurst, Some Application of Differential Thermal Analysis to Oils and Fats, *J. Food Technol. 1*:237–247 (1966).
26. Tunick, M.H., and E.L. Malin, Differential Scanning Calorimetry of Water Buffalo and Cow Milk Fat in Mozzarella Cheese, *J. Am. Oil Chem. Soc. 74*:1565–1568 (1997).
27. Che Man, Y.B., T. Haryati, H.M. Ghazali, and B.A. Asbi, Composition and Thermal Profile of Crude Palm Oil and Its Products, *Ibid. 76*:237–242 (1999).
28. AOCS, *Official Methods and Recommended Practices of the American Oil Chemists' Society*, 4th edn., edited by D. Firestone, AOCS Press, Champaign, IL, 1993.
29. Haryati, T., Y.B. Che Man, H.M. Ghazali, B.A. Asbi, and L. Buana, Determination of Iodine Value of Palm Oil Based on Triglyceride Composition, *J. Am. Oil Chem. Soc. 75*:789–792 (1998).
30. Stefanoudaki, E., F. Kotsifaki, and A. Koutsaftakis, The Potential of HPLC Triglyceride Profiles for the Classification of Cretan Olive Oils, *Food Chem. 60*:425–432 (1997).
31. Singleton, J.A., and H.E. Pattee, Characterization of Peanut Oil Triacylglycerols by HPLC, GLC and EIMS, *J. Am. Oil Chem. Soc. 64*:534–538 (1987).
32. Parcerisa, J., M. Rafecas, A.I. Castellote, R. Codony, A. Farran, J. Garcia, A. Lopez, A. Romero, and J. Boatella, Influence of Variety and Geographical Origin on the Fraction of Hazelnuts (*Corylus avellana* L.) from Spain: Triacylglycerol Composition, *Food Chem. 40*:245–249 (1994).
33. 7 *Series/UNIX DSC7 Users Manual*, Software Version 4.0, PerkinElmer Corporation, Norwalk, CT, 1995.
34. SAS, *Statistical Analysis System User's Guide: Basic Statistics*, SAS Institute, Cary, NC, 1989.
35. deMan, J.M., and L. deMan, Differential Scanning Calorimetry Techniques in the Evaluation of Fats for the Manufacture of Margarine and Shortening [Abstract], *INFORM 5*:522 (1994).

[Received April 12, 1999; accepted September 30, 1999]